

Channel Estimation based on Gaussian Mixture Models with Structured Covariances

Benedikt Fesl, Michael Joham, Sha Hu[†], Michael Koller, Nurettin Turan, and Wolfgang Utschick
School of Computation, Information and Technology, Technical University of Munich, Germany

[†]Huawei Sweden Technologies AB, Lund, Sweden

Email: {benedikt.fesl, joham, michael.koller, nurettin.turan, utschick}@tum.de

[†]Email: hu.sha@huawei.com

Abstract—In this work, we propose variations of a Gaussian mixture model (GMM) based channel estimator that was recently proven to be asymptotically optimal in the minimum mean square error (MMSE) sense. We account for the need of low computational complexity in the online estimation and low cost for training and storage in practical applications. To this end, we discuss modifications of the underlying expectation-maximization (EM) algorithm, which is needed to fit the parameters of the GMM, to allow for structurally constrained covariances. Further, we investigate splitting the 2D time and frequency estimation problem in wideband systems into cascaded 1D estimations with the help of the GMM. The proposed cascaded GMM approach drastically reduces the complexity and memory requirements. We observe that due to the training on realistic channel data, the proposed GMM estimators seem to inherently perform a trade-off between saving complexity/parameters and estimation performance. We compare these low-complexity approaches to a practical and low cost method that relies on the power delay profile (PDP) and the Doppler spectrum (DS). We argue that, with the training on scenario-specific data from the environment, these practical baselines are outperformed by far with equal estimation complexity.

Index Terms—conditional mean channel estimation, Gaussian mixture models, machine learning, low-complexity, OFDM

I. INTRODUCTION

In recent years, machine learning (ML) has emerged as a powerful tool in order to meet the increasing requirements for channel estimation (CE) [1]. ML approaches for communications are designed as *end-to-end learning*, e.g. [2], or *model-aided learning*, e.g. [3], or a mixture of both. The basis for all ML methods is the construction of appropriate datasets for training. In this work, we focus on the idea that the dataset is tailored for a specific scenario/environment of a base station (BS) cell. Such environments have immanent characteristics (e.g., buildings, streets) that can be seen as a prior for the communication tasks that are performed in this cell. These characteristics can not be modeled, but ML methods trained on appropriate data have access to these priors by learning their underlying distribution within the data during training.

In [4], [5], a Gaussian mixture model (GMM) based channel estimator is introduced that is proven to be the asymptotically optimal conditional mean estimator (CME) for an infinite number of mixture components. Since the CME is

approximated by the GMM estimator that is fitted with training data from a specific BS environment, this is a model-aided learning approach. Although the channel estimator performs well also for a finite number of components, the evaluation of the GMM estimator might lead to a prohibitively large complexity and memory overhead. However, by introducing certain assumptions on the system model, reasonable structural approximations of the covariance matrix can be found, e.g., a Toeplitz or circulant structure [6]. In addition, the 2D estimation of a time-frequency channel can be decomposed by exploiting a Kronecker structure or by cascaded 1D estimation [7].

In contrast, practical approaches focus on low cost methods that depend on specific parameters that are simple to estimate, such as the power delay profile (PDP) and the Doppler spectrum (DS) [8], [9]. Exploiting the known relations of the time/frequency correlations and the DS/PDP by the Fourier transform using the Wiener–Khinchin theorem [10], one can evaluate an linear minimum mean square error (LMMSE) estimate with these parameters.

The contributions of this work are summarized as follows. We propose different low-complexity approaches of the GMM based channel estimator from [4], [5] for wideband channels. In particular, we constrain the respective covariance matrices of each component to circulant or Toeplitz matrices by discrete Fourier transform (DFT) based decompositions. Especially, the Toeplitz case, realized by specific projections in the underlying expectation-maximization (EM) algorithm, shows a strong performance close to the GMM estimator having unconstrained covariances with much more parameters. We then propose a 2×1 D estimator that performs cascaded 1D estimations of the time and frequency channels in the online phase. For this, we fit one GMM for each dimension separately in the offline phase. This approach drastically reduces the complexity and storage requirements. We compare the respective low cost approaches to an LMMSE estimator based on DS/PDP, which are computed with knowledge of the true instantaneous channel realization.

II. SYSTEM AND CHANNEL MODEL

We consider a single-input single-output (SISO) transmission in the spatial domain over a doubly-selective fading

This work was funded by Huawei Sweden Technologies AB, Lund.

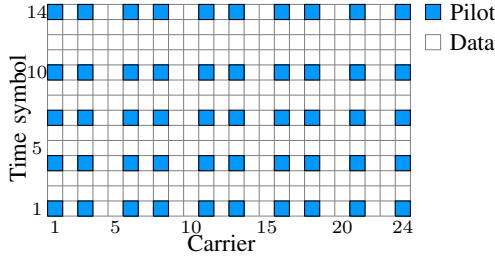


Fig. 1: Pilot allocation scheme of the lattice-type.

channel, where $\mathbf{H} \in \mathbb{C}^{N_c \times N_t}$ represents the time-frequency response of the channel for N_c subcarriers and N_t time slots. We consider a downlink (DL) frequency division duplex (FDD) system where the channel between uplink (UL) and DL is not reciprocal, but we can exploit the recently proposed distributional shift invariance of the UL and DL [11]. To this end, the training process can be performed centralized at the BS and the parameters are offloaded to the mobile terminal (MT), where the DL-CE is performed [12]. However, the proposed approaches are not limited to this and can be equivalently used in the UL and in a time division duplex (TDD) system.

When only N_p positions of the $N_t \times N_c$ time-frequency response are occupied by pilot symbols, there is a *selection matrix* $\mathbf{A} \in \{0, 1\}^{N_p \times N_c N_t}$ which represents the pilot positions. This leads to pilot observations

$$\mathbf{y} = \mathbf{A}\mathbf{h} + \mathbf{n} \in \mathbb{C}^{N_p} \quad (1)$$

with $\mathbf{h} = \text{vec}(\mathbf{H}) \in \mathbb{C}^{N_c N_t}$ and additive Gaussian noise $\mathbf{n} \sim \mathcal{N}_{\mathbb{C}}(\mathbf{0}, \mathbf{C}_n)$. In this work, we consider lattice-type pilots and the allocation scheme as shown in Fig. 1.

For the construction of a scenario-specific channel dataset, we use the QuaDRiGa channel simulator [13], [14]. QuaDRiGa models the channel of the c -th carrier and t -th time symbol as $H_{c,t} = \sum_{\ell=1}^L G_{\ell} e^{-2\pi j f_c \tau_{\ell,t}}$, where ℓ is the path number and L the number of multi-path components. The frequency of the c -th carrier is denoted by f_c and the ℓ -th path delay of the t -th time symbol by $\tau_{\ell,t}$. The coefficient G_{ℓ} comprises the attenuation of a path, the antenna radiation pattern weighting, and the polarization. We consider an urban macrocell (UMa) scenario following the 3GPP 38.901 specification, where the BS is placed at height of 25m and covers a sector of 120°. Each MT is either placed indoor (80%) or outdoor (20%) and moves with a certain velocity v in a random direction, which is captured by a drifting model. The generated channels are post-processed to remove the path gain [14].

III. POWER DELAY PROFILE AND DOPPLER SPECTRUM

Practical CE requires low complexity and memory overhead. To this end, it is beneficial to estimate the channel based on parameters that are simple to measure in practice, such as PDP and DS [8], [9]. Many works have considered estimating the PDP and DS for specific system and channel models. In this work, we assess the instantaneous PDP and DS by evaluating

the true underlying channel realization from the QuaDRiGa simulator. We calculate the instantaneous genie-PDP \mathbf{p}_i of the i th time symbol $\mathbf{h}_i \in \mathbb{C}^{N_c}$ (i.e., the i th column of \mathbf{H}) and the genie-DS \mathbf{d}_k of the k th carrier \mathbf{g}_k (i.e., the k th column of \mathbf{H}^T) as $\mathbf{p}_i = |\mathbf{F}_{N_c}^H \mathbf{h}_i|^2$ and $\mathbf{d}_k = |\mathbf{F}_{N_t} \mathbf{g}_k|^2$, where \mathbf{F}_M is the $M \times M$ DFT matrix and $|\cdot|$ denotes the element-wise magnitude. This approach is clearly utopian since the true channel that has to be estimated is used. However, in this way, we get a best-possible performance evaluation that can not be outperformed by estimating the PDP and DS.

Once these parameters are computed, the instantaneous frequency and time covariance matrices of the channel can be obtained due to the Wiener-Khinchin theorem [10] as $\mathbf{C}_i^{\text{PDP}} = \mathbf{F}_{N_c} \text{diag}(\mathbf{p}_i) \mathbf{F}_{N_c}^H$ and $\mathbf{C}_k^{\text{DS}} = \mathbf{F}_{N_t}^H \text{diag}(\mathbf{d}_k) \mathbf{F}_{N_t}$, respectively, where $\mathbf{C}_i^{\text{PDP}}$ and \mathbf{C}_k^{DS} denote the frequency and time covariance matrix according to the i th time symbol and k th carrier. These covariance estimates can now be used for evaluating the well-known LMMSE formula for subsequent 1D estimation of the frequency and time domain or by 2D estimation via the Kronecker product $\mathbf{C}^{\text{PDP}} \otimes \mathbf{C}^{\text{DS}}$ where the PDP (DS) is averaged over the N_t (N_c) time symbols (carriers).

IV. PROPOSED LOW-COMPLEXITY ESTIMATORS

We briefly introduce the GMMs and the CME based thereon from [4], [5]. A GMM with K components is a probability density function (PDF) of the form $f_{\mathbf{h}}^{(K)}(\mathbf{h}) = \sum_{k=1}^K p(k) \mathcal{N}_{\mathbb{C}}(\mathbf{h}; \boldsymbol{\mu}_k, \mathbf{C}_k)$ consisting of a weighted sum of K Gaussian PDFs [15, Sec. 9.2]. The probabilities $p(k)$ are called *mixing coefficients*, and $\boldsymbol{\mu}_k$ and \mathbf{C}_k denote the mean vector and covariance matrix of the k th GMM component, respectively. As explained in [15, Sec. 9.2], GMMs allow to calculate the *responsibilities* $p(k | \mathbf{h})$ by evaluating Gaussian likelihoods.

Given data samples, an EM algorithm can be used to fit a K -components GMM [15, Sec. 9.2]. At this point, we want to explicitly highlight the fact that GMMs are able to approximate any continuous PDF arbitrarily well [16]. In [4], [5], a CME is formulated based on GMMs, which is proven to asymptotically converge to the true CME when K grows large. The estimator is formulated as a weighted sum of LMMSE terms, given as

$$\hat{\mathbf{h}}^{(K)} = \sum_{k=1}^K p(k | \mathbf{y}) (\boldsymbol{\mu}_k + \mathbf{C}_k \mathbf{A}^H \mathbf{C}_{\mathbf{y},k}^{-1} (\mathbf{y} - \mathbf{A} \boldsymbol{\mu}_k)) \quad (2)$$

where the responsibilities $p(k | \mathbf{y})$ are computed by

$$p(k | \mathbf{y}) = \frac{p(k) \mathcal{N}_{\mathbb{C}}(\mathbf{y}; \mathbf{A} \boldsymbol{\mu}_k, \mathbf{C}_{\mathbf{y},k})}{\sum_{i=1}^K p(i) \mathcal{N}_{\mathbb{C}}(\mathbf{y}; \mathbf{A} \boldsymbol{\mu}_i, \mathbf{C}_{\mathbf{y},i})} \quad (3)$$

with $\mathbf{C}_{\mathbf{y},k} = \mathbf{A} \mathbf{C}_k \mathbf{A}^H + \mathbf{C}_n$. We denote the estimator that evaluates (2) for unrestricted covariance matrices as *GMM full*.

A. Toeplitz Estimator

In the considered system model with a constant carrier-spacing and time-sampling, the frequency- and time-domain

covariance matrices can be reasonably approximated by a Toeplitz matrix, respectively. Thus, for the vectorized channel, the covariance matrix resembles a block-Toeplitz matrix with Toeplitz blocks. The class of channel covariance matrices that are expressed as

$$\mathbf{C} = \tilde{\mathbf{Q}}^H \text{diag}(\mathbf{c}) \tilde{\mathbf{Q}} \in \mathbb{C}^{N_c N_t \times N_c N_t} \quad (4)$$

are exactly the positive-definite Hermitian block-Toeplitz matrices with Toeplitz blocks, where $\tilde{\mathbf{Q}} = \mathbf{Q}_{N_t} \otimes \mathbf{Q}_{N_c}$. Further, \mathbf{Q}_M contains the first M columns of a $2M \times 2M$ DFT matrix, and $\mathbf{c} \in \mathbb{R}_+^{4N_c N_t}$ [17]. The description of a Toeplitz-structured covariance matrix in (4) exactly refers to the form that is investigated in [18] for covariance estimation using the EM algorithm. That is, we can apply the derived matrix transformations in the M-step in order to have the desired structured covariances in the GMM. In the unconstrained case, the update of the covariance matrix of the k th component in the M-step of the i th EM iteration is computed by means of the sample covariance matrix $\hat{\mathbf{C}}_k^{(i)}$. However, as suggested in [18], if the resulting covariance matrix $\mathbf{C}_k^{(i+1)}$ has the form of (4), the update of the covariance matrix in the M-step is

$$\mathbf{C}_k^{(i+1)} = \tilde{\mathbf{Q}}^H \text{diag}(\mathbf{c}_k^{(i+1)}) \tilde{\mathbf{Q}}, \quad (5)$$

$$\mathbf{c}_k^{(i+1)} = \mathbf{c}_k^{(i)} + \text{diag} \left(\text{diag}(\mathbf{c}_k^{(i)}) \boldsymbol{\Theta}_k^{(i)} \text{diag}(\mathbf{c}_k^{(i)}) \right), \quad (6)$$

$$\boldsymbol{\Theta}_k^{(i)} = \tilde{\mathbf{Q}} \left(\mathbf{C}_k^{(i),-1} \hat{\mathbf{C}}_k^{(i)} \mathbf{C}_k^{(i),-1} - \mathbf{C}_k^{(i),-1} \right) \tilde{\mathbf{Q}}^H. \quad (7)$$

After the fitting process, only the diagonal vectors \mathbf{c}_k for $k = 1, \dots, K$ have to be stored. The computation of matrix-vector products with $\tilde{\mathbf{Q}}$ can be performed by applying 2D fast Fourier transforms (FFTs), yielding complexity savings as discussed later. We refer to this estimator as *GMM b-toep*.

B. Circulant Estimator

Toeplitz matrices are asymptotically equivalent to corresponding circulant matrices, cf. [6]. The approximation with circulant covariance matrices is less general than the Toeplitz approximation, but allows for further simplifications. It is well-known that the class of block-circulant matrices is diagonalized by the 2D-DFT matrix $\mathbf{F}_{N_t, N_c} = \mathbf{F}_{N_t} \otimes \mathbf{F}_{N_c}$, i.e., $\mathbf{C} = \mathbf{F}_{N_t, N_c}^H \text{diag}(\mathbf{c}) \mathbf{F}_{N_t, N_c}$, where $\mathbf{c} \in \mathbb{R}_+^{N_c N_t}$. Similarly explained in [5], this allows for fitting a GMM with diagonal covariances to 2D-DFT transformed data samples and thus obtaining a GMM of the original data with circulant covariance matrices as stated above and the means via $\mathbf{F}_{N_t, N_c}^H \boldsymbol{\mu}_k$. Note that this procedure can only be done because the DFT matrices are unitary, which does not hold for the transformation matrix in (4). Thus, the fitting with diagonal covariances in the GMM simplifies the training compared to the transformations in (5)–(7) with full matrices. We refer to this estimator as *GMM b-circ*.

C. Kronecker Estimator

If it is assumed that the covariance matrix of the time-frequency channel is separable, it can be decomposed via the Kronecker product, i.e., $\mathbf{C} = \mathbf{C}^{\text{time}} \otimes \mathbf{C}^{\text{freq}}$. This allows for

fitting two separate GMMs with K_t (and K_c) components that are purely trained with the rows (columns) of the channel matrix \mathbf{H} for the time (frequency) covariance matrix \mathbf{C}^{time} (\mathbf{C}^{freq}). Afterwards, the high-dimensional covariance matrix is evaluated by combinatorial computation of the Kronecker products of all components to obtain the high-dimensional GMM with $K_c K_t$ components. The same is done for the GMM means and the mixing coefficients are evaluated by performing a single E-step of the EM algorithm. This is similarly presented in [5] for MIMO channels and is explained here briefly for completeness. We refer to this estimator as *GMM kron*.

D. 2×1D Estimator

As stated firstly in [7] and used later on in various applications, the 2D LMMSE filter can be decomposed into cascaded 1D filters with only marginal performance losses, yet greatly decreasing the memory and complexity overhead. Thereby, the ordering of estimating first in frequency or time domain is arbitrary due to linearity. Similarly as in the Kronecker estimator, two GMMs are fitted for the time and frequency domain by splitting the channel matrix into rows and columns. However, instead of computing high-dimensional covariance matrices afterwards, CE is performed by successively evaluating the LMMSE formula for each row and column of the 2D channel matrix, respectively. The number of pilots in the time and frequency dimensions are N_{pt} and N_{pc} , respectively, yielding $N_p = N_{pt} N_{pc}$ and $\mathbf{A} = \mathbf{A}_t \otimes \mathbf{A}_c$ with $\mathbf{A}_t \in \{0, 1\}^{N_{pt} \times N_t}$ and $\mathbf{A}_c \in \{0, 1\}^{N_{pc} \times N_c}$. Consequently, the system model in (1) can be split into a time and frequency observation by replacing \mathbf{A} with \mathbf{A}_t and \mathbf{A}_c , as well as replacing the vectorized channel with a row and column of \mathbf{H} . After evaluating the likelihood of the time and frequency GMM, each row and column is estimated separately via the LMMSE formula in a successive manner. We refer to this estimator as *GMM 2×1D*. By constraining the covariances of each low-dimensional GMM further to a Toeplitz or circulant structure, additional memory and complexity overhead can be saved. For the Toeplitz and circulant case, the same procedure as in Sec. IV-A and IV-B is adopted by replacing the 2D- by 1D-DFT matrices. We refer to these estimators as *GMM 2×1D-toep* and *GMM 2×1D-circ*.

E. Memory and Complexity Analysis

The parameters of a GMM are determined by the covariance matrices, the means and the mixing coefficients. The number of parameters for each variant are displayed in Table 1 and are explicitly computed for the setting in Sec. V as discussed later. The parameter number is especially important for the FDD case where the parameters that are learned centralized at the BS have to be offloaded to the MTs as reasoned in Sec. II.

The online complexity of the different approaches is determined by evaluating the responsibilities (3) and the weighted LMMSE sum (2). Because the mixture components are fixed after training, this allows for pre-computing the filters, including the inverses of $\mathbf{C}_{y,k}$, in an offline phase for each

Name	Parameters	Example
full	$K(\frac{1}{2}N_c^2N_t^2 + 2N_cN_t + 1)$	$7.29 \cdot 10^6$
kron	$K_c(\frac{1}{2}N_c^2 + 2N_c + 1) + K_t(\frac{1}{2}N_t^2 + 2N_t + 1)$	$5.78 \cdot 10^3$
b-toep	$K(5N_cN_t + 1)$	$2.15 \cdot 10^5$
b-circ	$K(2N_cN_t + 1)$	$8.61 \cdot 10^4$
$2 \times 1D$	$K_c(\frac{1}{2}N_c^2 + 2N_c + 1) + K_t(\frac{1}{2}N_t^2 + 2N_t + 1)$	$3.39 \cdot 10^4$
$2 \times 1D$ -toep	$K_c(5N_c + 1) + K_t(5N_t + 1)$	$1.39 \cdot 10^4$
$2 \times 1D$ -circ	$K_c(2N_c + 1) + K_t(2N_t + 1)$	$5.63 \cdot 10^3$

Table 1: Parameters of the GMM-based approaches. The example numbers are computed for the setting in Sec. V.

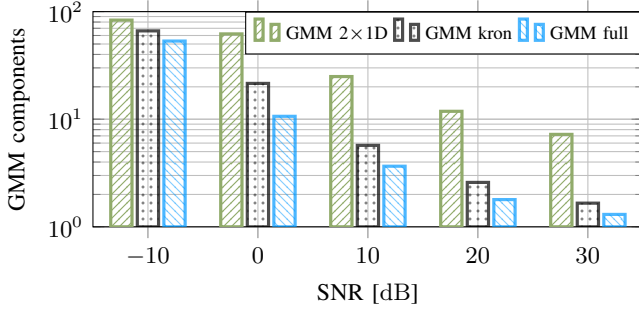


Fig. 2: Average number of GMM components necessary to achieve 99% responsibility for MTs with $v \in [0; 300]$ km/h.

signal-to-noise ratio (SNR). It has to be noted here that it is generally not necessary to compute the whole sum in (2), but only a small fraction of it per sample, dependent on the SNR, as shown later. Due to the generally unstructured noise covariance C_n and the selection matrix A , the structurally constrained cases do not directly translate into a lower online complexity. However, in the case of white noise with $C_n = \sigma^2 \mathbf{I}$, complexity can be saved by using the Sherman–Morrison formula for computing the inverse of $C_{y,k} = A Q^H \text{diag}(c + \sigma^2 \mathbf{1}) Q A^H$ that first inverts the large matrix $Q^H \text{diag}(c + \sigma^2 \mathbf{1}) Q$, which is simple, and afterwards finds the inverse of the submatrix [19]. If the whole filters for each SNR value are not pre-computed, the (block-)circulant and (block-)Toeplitz approaches clearly allow for substantial complexity savings due to the FFTs. The approaches utilizing the PDP/DS depend on the instantaneous channel realizations and do not allow for pre-computations.

V. NUMERICAL RESULTS

We conducted numerical experiments for the discussed system and channel model from Sec. II with $N_c = 24$, $N_t = 14$ and $N_p = 50$, cf. Fig. 1. We assume $C_n = \sigma^2 \mathbf{I}$. The channels are normalized such that $E[\|h\|_2^2] = N_c N_t$, and the SNR is defined as $1/\sigma^2$. The MSE between the true and estimated channel is normalized by $N_c N_t$. The amount of training and test data is 10^5 and 10^4 , respectively. The 2D GMMs have $K = 128$ components. For *GMM kron* and *GMM $2 \times 1D$* , the time and frequency domain GMMs have ($K_t = 8$,

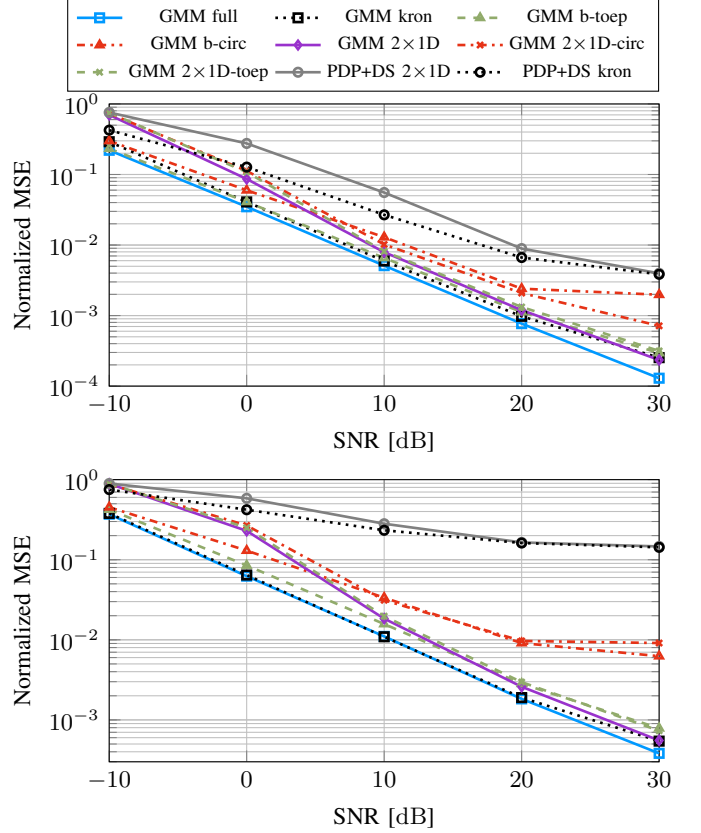


Fig. 3: Channel estimation performance for MTs with $v = 3$ km/h (top) and $v \in [0; 300]$ km/h (bottom).

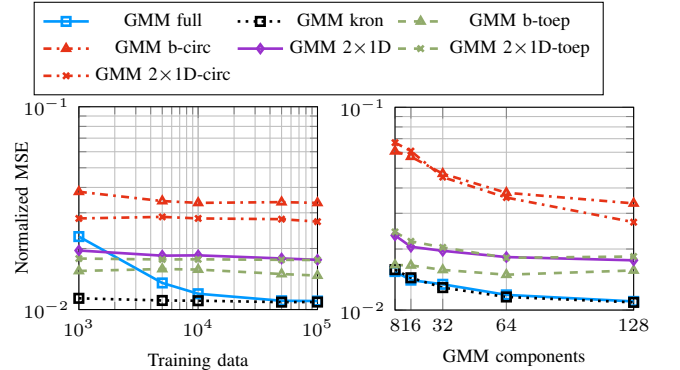


Fig. 4: Estimation performance of the GMM-based approaches for varying numbers of training samples (left) and components (right) with $v \in [0; 300]$ km/h and SNR = 10 dB.

$K_c = 16$) and ($K_t = 32, K_c = 96$) components, respectively, such that their respective product and sum yield again 128 components.

For this setting, the parameters in Table 1 reveal that *GMM b-toep* and *GMM b-circ* only need approximately 3% and 1% parameters compared to *GMM full*, respectively, and *GMM $2 \times 1D$* needs less than 0.5%. Most remarkably, *GMM kron* and *GMM $2 \times 1D$ -circ* need less than 0.01% parameters as

compared to *GMM full*.

Since $\sum_{k=1}^K p(k | \mathbf{y}) = 1$, cf. (3), we evaluate the necessary mean number of GMM components that is needed to achieve at least 99% responsibility in the online estimation. In Fig. 2, it can be observed that for higher SNR values, the number of components can be reduced drastically. A reason for this is that in low SNR, the noise variance dominates in $\mathbf{C}_{\mathbf{y},k}$ from (3) and hence, there is higher uncertainty which component is most likely to be responsible for the underlying channel realization. Additionally, *GMM kron* and *GMM 2×1D* need a higher number of components than *GMM full*. This can be similarly reasoned, since the additional assumptions do not hold in general and thus contribute to the uncertainty. As a result, the GMM appears to inherently perform a trade-off between more components for estimation and less parameters/complexity.

In Fig. 3, we compare the GMM variants and the PDP/DS based estimators with respect to their MSE performance for different SNR values. In the upper plot, we conducted simulations with MTs that have a fixed velocity of 3km/h. As expected, *GMM full* yields the best performance, closely followed by *GMM kron* and *GMM b-toep* with negligible losses for low to medium SNR values and an increasing gap for higher SNR values. *GMM b-circ* has a large gap for higher SNR values, where it saturates. *GMM 2×1D* has a larger gap to *GMM full* in the low SNR range compared to the 2D estimators, but performs similarly well as *GMM kron* for higher SNR values. Remarkably, *GMM 2×1D-toep* has negligible loss to *GMM 2×1D* over the whole SNR range, whereas *GMM 2×1D-circ* again shows an increasing performance gap for higher SNR values. The 2×1D estimator based on PDP/DS is outperformed substantially by all GMM approaches over the whole SNR range. The Kronecker based estimator with PDP/DS is only better than the 2×1D GMM estimators in the low SNR range due to the higher online complexity. However, for higher SNR values it is outperformed by all GMM variants.

In the bottom plot of Fig. 3, each MT in the cell moves with a velocity that is randomly sampled between 0–300km/h (in both the training and test data). The findings for the GMM based estimators are in agreement with the results for a fixed $v = 3\text{km/h}$. However, the performance gap of the circulant based estimators increases in the higher SNR range. The PDP/DS based estimators show a very poor performance with drastic losses as compared to the GMM based approaches. To conclude, the GMM estimators, even when having low online complexity and few parameters due to the structural constraints, outperform the estimators based on PDP and DS (evaluated with the ground truth channel) by far in both settings. This can be reasoned with the ability of the GMM to utilize the prior information about the scenario/environment, including side information such as the MT’s mobility.

In the left plot of Fig. 4, we compare the GMM variants for different numbers of training data for MTs with random velocity between 0–300km/h and SNR of 10dB. The low-complexity approaches, due to their drastically reduced number of parameters, cf. Table 1, are already converging

for 10^3 training samples, whereas *GMM full* needs around 10^5 training samples until convergence. This underlines the practical importance of the structurally constrained estimators. In the right plot of Fig. 4, we compared the GMM approaches for the same setting as before for different number of components. *GMM kron* and *GMM 2×1D* always yield the equivalent amount of components when multiplied or summed, respectively. As expected, the MSE decreases for higher number of components. It can be observed that the performance saturates at around 64 to 128 components, except for the (block-)circulant approaches. To summarize, increasing the number of components has the most impact on the ultra-low complexity methods with a saturation effect for higher number of components.

VI. CONCLUSION

In this work, we proposed structurally constrained GMM based channel estimators that are designed for a specific scenario/environment. As a key result, a great amount of parameters and computational complexity can be saved with only small performance losses. A special mentioning deserves the Toeplitz based estimator that shows the best trade-off between parameters/complexity and performance. In comparison with a PDP/DS based estimator that is evaluated with the instantaneous ground truth data, the GMM based approaches are clearly superior in performance due to their ability to adapt to the present environment and access this as a prior information.

REFERENCES

- [1] H. Ye, G. Y. Li, and B.-H. Juang, “Power of Deep Learning for Channel Estimation and Signal Detection in OFDM Systems,” *IEEE Commun. Lett.*, vol. 7, no. 1, pp. 114–117, 2018.
- [2] H. Ye, L. Liang, G. Y. Li, and B.-H. Juang, “Deep Learning-Based End-to-End Wireless Communication Systems With Conditional GANs as Unknown Channels,” *IEEE Trans. Wireless Commun.*, vol. 19, no. 5, pp. 3133–3143, 2020.
- [3] D. Neumann, T. Wiese, and W. Utschick, “Learning the MMSE Channel Estimator,” *IEEE Trans. Signal Process.*, vol. 66, no. 11, pp. 2905–2917, 2018.
- [4] M. Koller, B. Fesl, N. Turan, and W. Utschick, “An Asymptotically Optimal Approximation of the Conditional Mean Channel Estimator Based on Gaussian Mixture Models,” in *2022 IEEE Int. Conf. on Acoust., Speech and Signal Process.*, 2022, pp. 5268–5272.
- [5] —, “An Asymptotically MSE-Optimal Estimator based on Gaussian Mixture Models,” *IEEE Trans. Signal Process.*, 2022.
- [6] R. M. Gray, “Toeplitz and Circulant Matrices: A Review,” *Found. Trends Commun. Inf. Theory*, vol. 2, no. 3, pp. 155–239, 2006.
- [7] P. Hoeher, S. Kaiser, and P. Robertson, “Two-Dimensional Pilot-Symbol-Aided Channel Estimation by Wiener Filtering,” in *IEEE Int. Conf. on Acoust., Speech and Signal Process.*, vol. 3, 1997, pp. 1845–1848 vol.3.
- [8] Y.-J. Kim and G.-H. Im, “Pilot-Symbol Assisted Power Delay Profile Estimation for MIMO-OFDM Systems,” *IEEE Commun. Lett.*, vol. 16, no. 1, pp. 68–71, 2012.
- [9] M. Cicerone, O. Simeone, and U. Spagnolini, “Channel Estimation for MIMO-OFDM Systems by Modal Analysis/Filtering,” *IEEE Trans. Wireless Commun.*, vol. 54, no. 11, pp. 2062–2074, 2006.
- [10] C. Chatfield, *The Analysis of Time Series - An Introduction*. Chapman and Hall/CRC, 1989.
- [11] W. Utschick, V. Rizzello, M. Joham, Z. Ma, and L. Piazzi, “Learning the CSI Recovery in FDD Systems,” *IEEE Trans. Wireless Commun.*, 2022.

- [12] B. Fesl, N. Turan, M. Koller, M. Joham, and W. Utschick, "Centralized Learning of the Distributed Downlink Channel Estimators in FDD Systems using Uplink Data," in *25th Int. ITG Workshop on Smart Antennas*, 2021.
- [13] S. Jaeckel, L. Raschkowski, K. Börner, and L. Thiele, "QuaDRiGa: A 3-D Multi-Cell Channel Model With Time Evolution for Enabling Virtual Field Trials," *IEEE Trans. Antennas Propag.*, vol. 62, no. 6, pp. 3242–3256, 2014.
- [14] S. Jaeckel, L. Raschkowski, K. Börner, L. Thiele, F. Burkhardt, and E. Eberlein, "QuaDRiGa: Quasi Deterministic Radio Channel Generator, User Manual and Documentation," Fraunhofer Heinrich Hertz Institute, Tech. Rep., v2.2.0, 2019.
- [15] C. M. Bishop, *Pattern Recognition and Machine Learning (Information Science and Statistics)*. Berlin, Heidelberg: Springer-Verlag, 2006.
- [16] T. T. Nguyen, H. D. Nguyen, F. Chamroukhi, and G. J. McLachlan, "Approximation by Finite Mixtures of Continuous Density Functions that Vanish at Infinity," *Cogent Math. Statist.*, vol. 7, no. 1, p. 1750861, 2020.
- [17] G. Strang, "A Proposal for Toeplitz Matrix Calculations," *Studies in Applied Mathematics*, vol. 74, no. 2, pp. 171–176, 1986.
- [18] T. Barton and D. Fuhrmann, "Covariance Estimation for Multidimensional Data using the EM Algorithm," in *Proc. of 27th Asilomar Conf. on Signals, Syst. and Comput.*, 1993, pp. 203–207.
- [19] E. J. Ruiz, R. C. Maldonado, and F. P. Rodríguez, "Relationship between the Inverses of a Matrix and a Submatrix," *Computación y Sistemas*, 2016.